Design and Analysis of a Radio-over-Fiber System for Cloud Radio Access Network

A Term Project Report

Submitted by

Aditya Dhote (252CN004)
Harish Arjun (252CN018)

in partial fulfillment of the requirements for the degree of

MASTER OF TECHNOLOGY

In

COMMUNICATION ENGINEERING AND NETWORKS

Under the Guidance of

Dr. Mandeep Singh

DEPARTMENT OF ELECTRONICS AND COMMUNICATION

NATIONAL INSTITUTE OF TECHNOLOGY KARNATAKA

SURATHKAL, MANGALORE- 575025

Table of Contents

Abstract

This project presents the design and performance analysis of a dual-channel Radio-over-Fibre (RoF) system operating at 28 GHz for 5G fronthaul applications in a Cloud Radio Access Network (C-RAN) architecture. The primary objective is to evaluate the system's capability to deliver high frequency millimeter wave (mmWave) signals over a 20 km optical fibre link while maintaining acceptable signal quality. The proposed RoF link is designed and simulated to assess performance with optical amplification by analyzing key parameters such as received optical power.

The project also highlights the critical influence of fibre dispersion on signal integrity, demonstrating that chromatic dispersion becomes a dominant limiting factor beyond power enhancement effects from amplification. Although amplification improves received power and extends transmission reach, dispersion-induced distortion continues to degrade system performance, particularly at higher frequencies and data rates.

The analysis provides insights into the balance between optical power management and dispersion control required for reliable mmWave RoF transmission. Future improvements are suggested through the integration of dispersion compensation techniques, such as dispersion-compensating fibres or digital pre-compensation, and the suppression of unwanted harmonic components to further enhance system fidelity. Overall, the results establish a foundational understanding of the performance trade-offs in 28 GHz RoF systems and support the feasibility of RoF as a promising fronthaul technology for high-capacity 5G C-RAN deployments.

CHAPTER 1: Introduction

5G represents the latest generation of mobile communication technology, designed to deliver ultra-fast data rates, reduced latency, and support for advanced applications such as intelligent transportation systems and real-time control. To achieve these capabilities, 5G leverages new frequency bands, including millimeter waves (30–300 GHz), but this advancement also places higher demands on network infrastructure, particularly the fronthaul link that connects centralized Baseband Units (BBUs) to distributed Remote Radio Heads (RRHs). Radio-over-Fibre (RoF) has emerged as an effective solution to these fronthaul challenges by transmitting radio frequency (RF) signals through optical fibre. Compared with conventional copper or coaxial cables, optical fibre provides exceptionally low signal attenuation, large bandwidth, and immunity to electromagnetic interference.

As a result, RF signals can be transmitted over longer distances with minimal degradation, improving signal-to-noise ratio (SNR). RoF also facilitates centralized BBU control while enabling RRHs to be deployed flexibly in remote or high-density locations, thereby enhancing scalability and network efficiency. Previous research has investigated RoF systems employing millimeter-wave signals to meet the requirements of 5G fronthaul. A key challenge in such systems is signal dispersion, which can impact transmission quality over extended distances. Dispersion compensating fibre (DCF) mitigates this issue by restoring signal integrity. To further increase capacity, Wavelength Division Multiplexing (WDM) is employed, allowing multiple signals to be transmitted on separate wavelengths.

Amplifiers are equally important in offsetting transmission losses and maintaining signal quality. The choice of amplification technology and modulation scheme greatly influences system performance. Among the available solutions, Semiconductor Optical Amplifiers (SOAs) have demonstrated strong potential, as recent design improvements have enhanced their efficiency and reliability. This study concentrates on optimizing a single-channel RoF system for 5G fronthaul at a 28 GHz millimeter-wave frequency. It examines the role of SOAs in mitigating power loss during fibre transmission. The findings indicate that SOAs significantly strengthen the received signal and improve the Q-factor.

CHAPTER 2: Objective

- To design and evaluate a dual-channel Radio-over-Fibre (RoF) system operating at 28 GHz for 5G fronthaul over a 20 km transmission distance.

- To investigate the system performance by analyzing received power.

- To assess the effectiveness of amplification in enhancing signal strength, while examining the influence of fibre dispersion as a key factor affecting data transmission quality.

- To identify the limitations of the proposed scheme, particularly the dominance of dispersion effects over power level in determining system performance.

- To explore potential future enhancements, including the use of dispersion compensation techniques and suppression of unwanted harmonic frequencies, to improve transmission quality and system reliability.

CHAPTER 3: Proposed Methodology

3.1 Implemented Transmitter Methodology

The proposed Radio-over-Fiber (RoF) system is designed to transport high-frequency wireless signals over a long-haul optical communication link while preserving the integrity of the digital information. The approach relies on intensity modulation and direct detection (IM/DD), where a 28 GHz RF carrier, carrying 1 Gbps digital data, is transparently mapped onto an optical carrier and transmitted over a 20 km single-mode optical fiber. The entire architecture is simulated and evaluated using OptiSystem software. This project simulates an optical carrier transmitting two RF signals with optical carrier suppression. An optical Mach-Zehnder modulator is used for both optical carrier suppression and signal modulation.

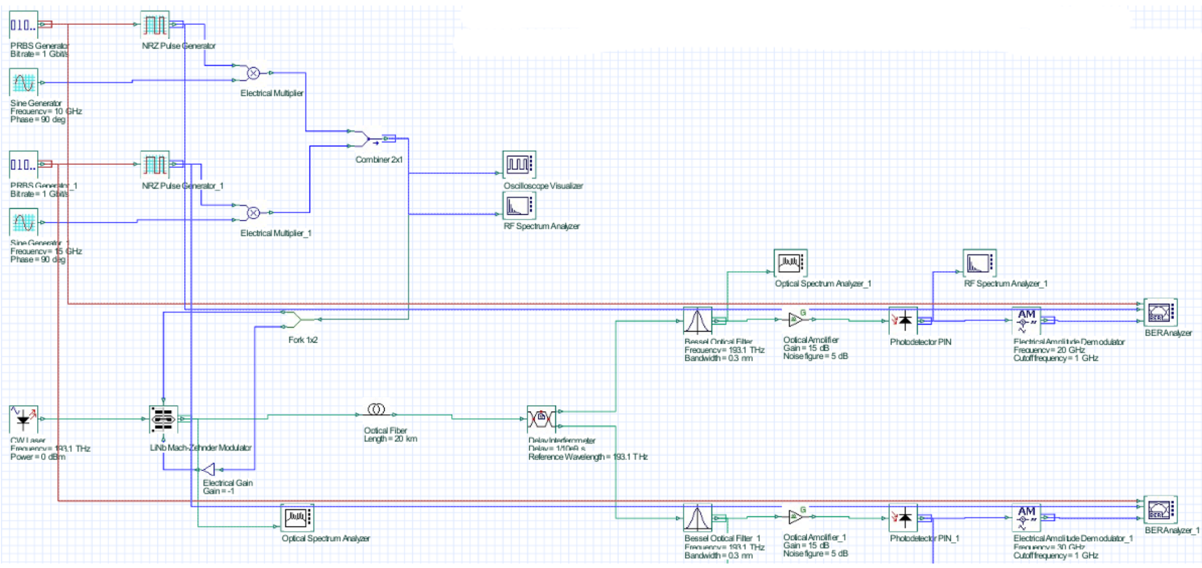

Figure 1: Implemented Schematic of the Proposed RoF System

The transmitter block as shown in Figure 1 begins with the generation of two independent data sequences using pseudo-random binary sequence (PRBS) generators. These digital streams are encoded using Non-Return-to-Zero (NRZ) pulse shaping to produce two 1 Gbps baseband signals. Each of these data streams modulates a 28 GHz sinusoidal carrier generated by RF oscillators. Electrical multipliers are used for this upconversion process, effectively producing binary amplitude-shift keyed (BASK) RF signals. Since the objective is to demonstrate a multi-service or multi-user

RoF transport scenario, these two independently modulated RF signals are combined using a 2×1 RF combiner.

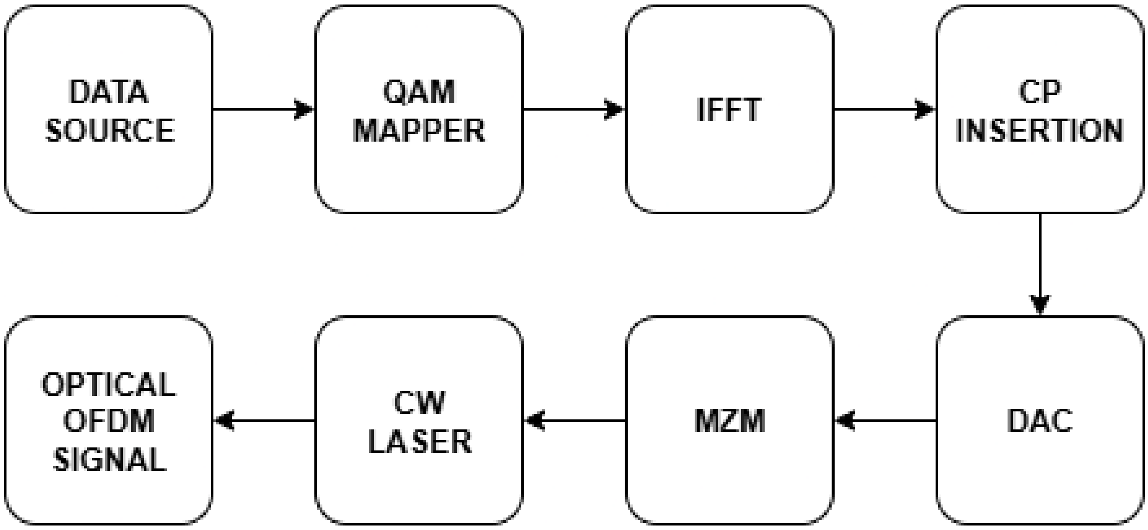

Figure 2: Block diagram of the transmitter

3.2 Implemented Transmission Methodology

The transmission link as shown in Figure 4 translates the electrical RF information into the optical domain, a continuous-wave (CW) laser operating at a frequency of 193.1 THz (corresponding to the standard 1550 nm wavelength range) is employed as the optical carrier source. The combined RF signal is fed into a Lithium-Niobate Mach–Zehnder Modulator (MZM), which performs intensity modulation by varying the optical output power proportionally to the input RF waveform. An electrical amplifier is used before the MZM to ensure that the drive voltage is strong enough to achieve efficient modulation. This process results in the generation of an optical signal that contains the original RF subcarrier as well as the embedded data, effectively accomplishing the RoF conversion process.

$$P(z) = P(0)\, e^{-\alpha z}$$

$$H_{CD}(f) = e^{-j\frac{\pi\lambda^2 DL}{c}f^2}$$

where alpha is the fiber loss coefficient and z is the transmission distance. To evaluate the impact of amplification, two transmission scenarios are considered. The modulated optical signal is then transmitted through a 20 km section of standard single-mode fiber (SMF). During propagation, the signal experiences fiber-induced impairments such as attenuation, chromatic dispersion, and phase noise, which can degrade the recovered signal

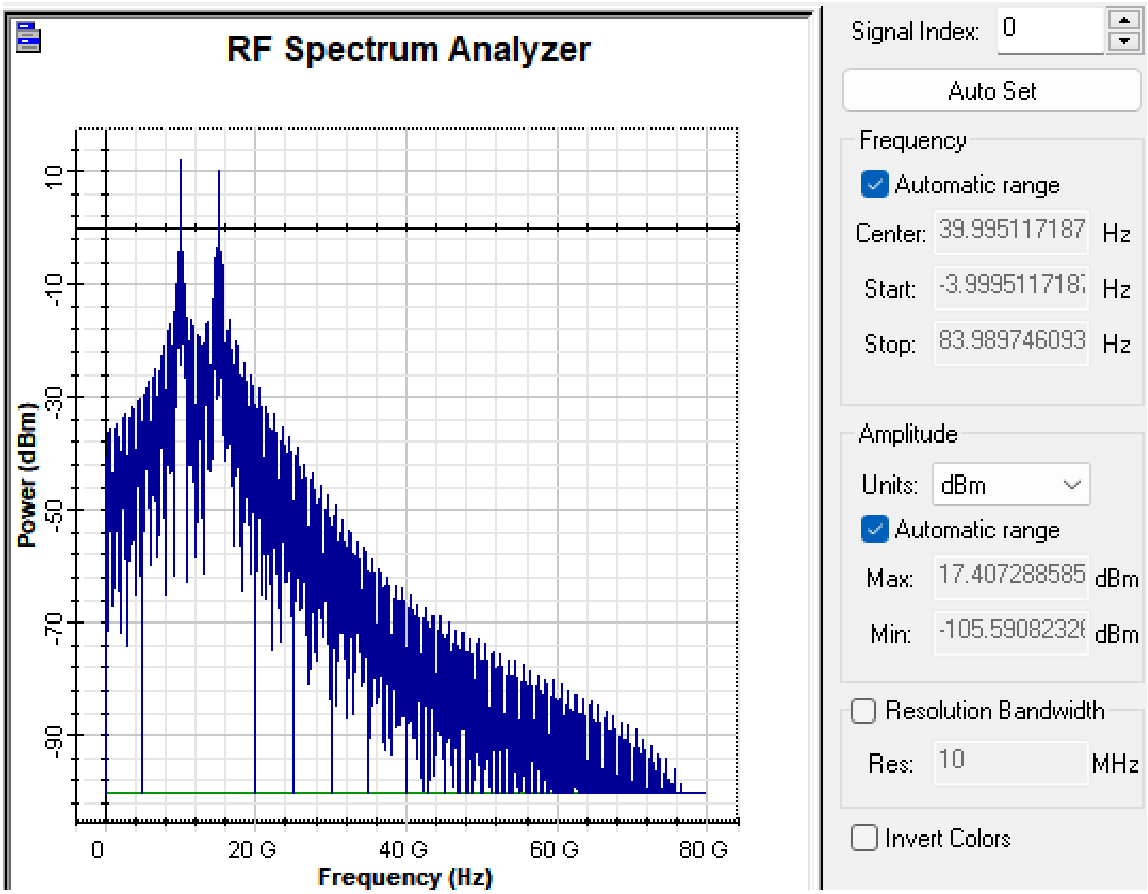

Figure 3: Spectrum of the Input Signal

quality at the receiver. An Optical Spectrum Analyzer is placed along the link to observe the evolution of the modulated optical spectrum, ensuring that the RF subcarriers are preserved even after fiber transmission.

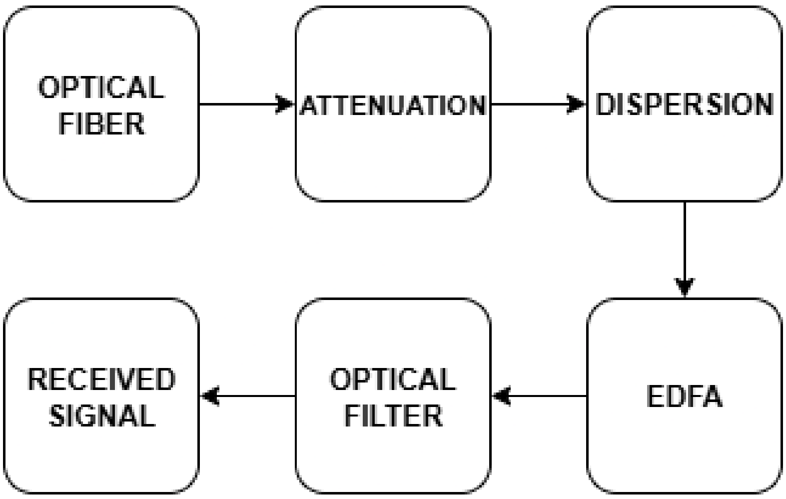

Figure 4: Block diagram of the transmission channel

3.3 Implemented Receiver Methodology

The receiver block as shown in Figure 5 is responsible for converting the optical signal back into the electrical domain and analyzing its quality. A photodetector, either PIN or Avalanche Photodiode (APD) is used to detect the incoming optical signal. The detector is selected based on its responsivity and bandwidth, ensuring it can accurately capture the 28 GHz signal components. The photodetector converts the optical OFDM signal into an electrical current proportional to the square of the optical field:

$$i(t) = R\,|E_{out}(t)|^2$$

where R is the responsivity of the photodiode.

Post-detection, the electrical signal is filtered using a bandpass filter centered at 28 GHz to isolate the desired frequency and suppress noise. An amplifier is then used to restore signal strength to measurable levels. The amplified signal is analyzed using eye diagram viewers, and RF spectrum analyzers within OptiSystem.

Key performance indicators such as received power and Q-factor are extracted and compared across both transmission scenarios. The results demonstrate that SOA inclusion significantly enhances received signal strength and improves Q-factor, indicating the need for further optimization through dispersion compensation or advanced modulation techniques.

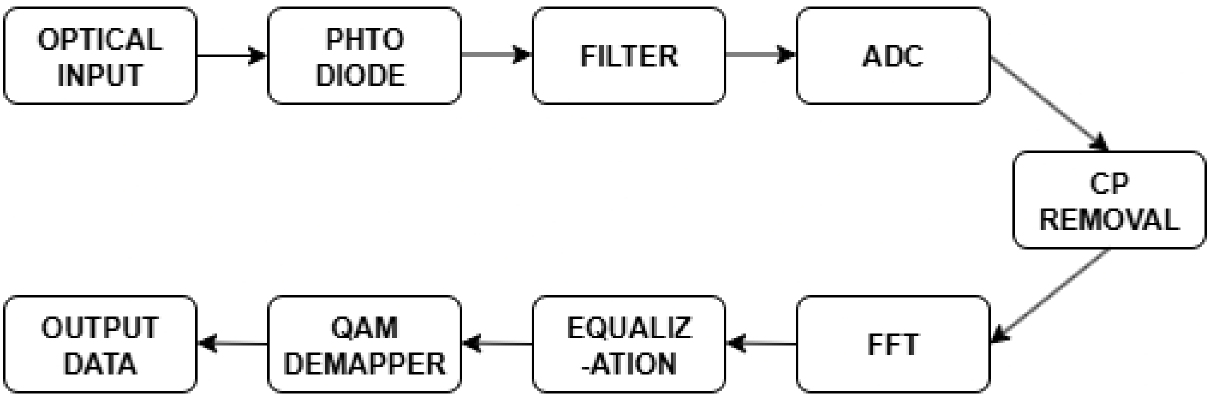

Figure 5: Block diagram of the receiver

CHAPTER 4: Simulation Result and Discussion

The optical communication system was simulated using a schematic comprising a CW laser, Mach-Zehnder modulator (MZM), 20 km optical fiber link, EDFA, and a receiver chain with a PIN photodetector, low-pass filter, and 3R regenerator. The CW laser as shown in Figure 6 is operated at 193.1 THz with 15.44 dBm output and produces a narrow spectral peak at 1552.5 nm. The MZM, with V = 4 V and bias = 2 V, effectively modulated the electrical signal onto the optical carrier, as confirmed by the RF Spectrum Analyzer showing a strong baseband signal and minimal harmonic distortion.

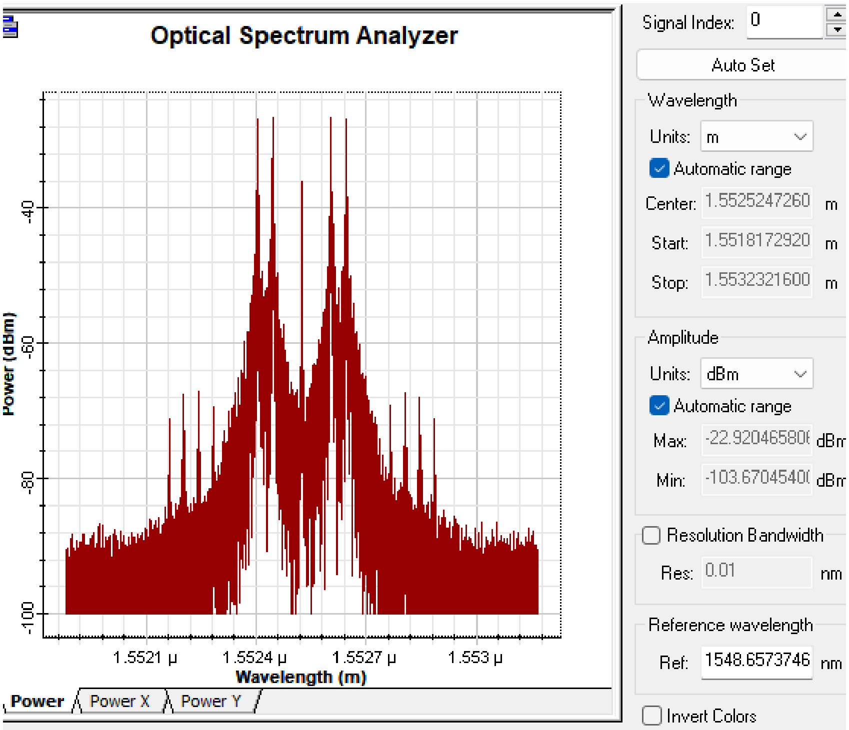

Figure 6: Optical Spectrum of CW Laser

The optical signal characterized by an attenuation of 0.2 dB/km, chromatic dispersion of 16.75 ps/nm/km, and a nonlinear refractive index of 2.6×10^{2} m^2/W. These parameters contributed to pulse broadening and power degradation, which were effectively mitigated by the inclusion of an EDFA with a gain of 10 dB and a noise figure of 5 dB. Post-amplification spectral analysis revealed broadened peaks and an elevated noise floor, consistent with amplified spontaneous emission (ASE) noise, yet the overall optical signal-to-noise ratio remained within acceptable limits for high-speed transmission.

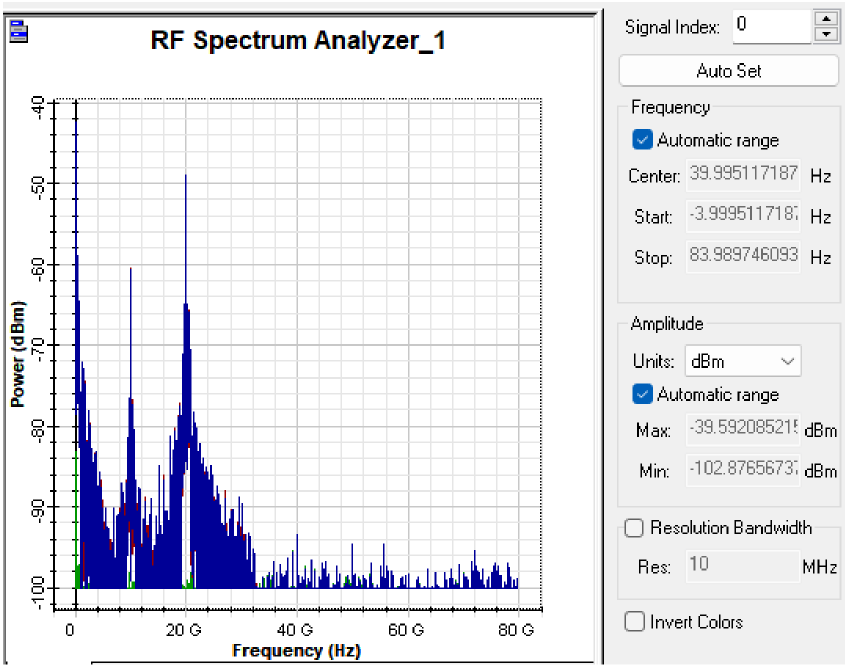

Figure 7: Spectrum of Output at PIN Diode 1

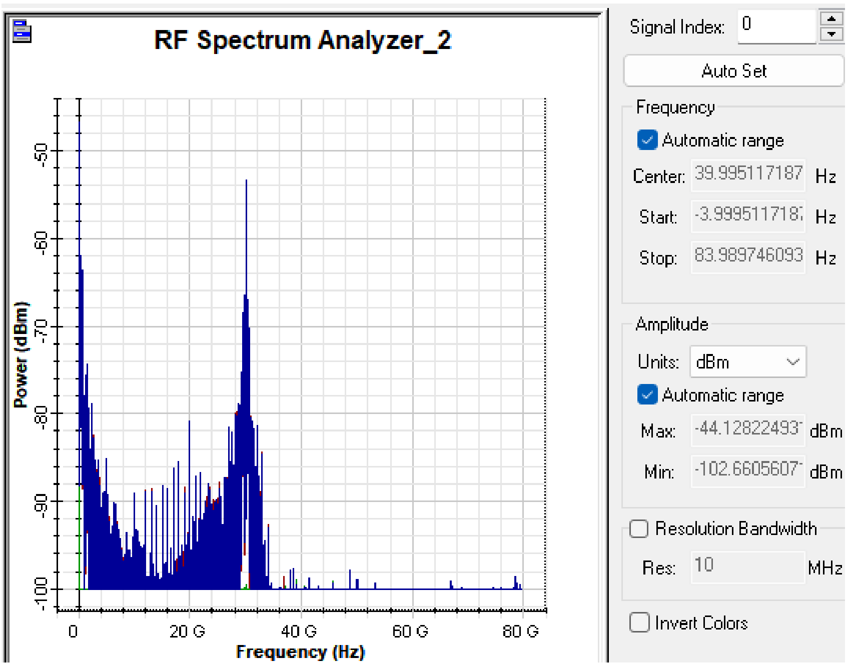

Figure 8: Spectrum of Output at PIN Diode 2

At the receiver end, the PIN photodetector with a responsivity of 1 A/W and a dark current of 10 nA provided efficient optical-to-electrical conversion. The subsequent low-pass filtering, with a cutoff frequency set to 0.75 times the bit rate (7.5 GHz for a 10 Gbps system), effectively suppressed high-frequency noise. The 3R regenerator restored signal amplitude, timing, and shape, ensuring reliable data recovery. The well-opened pattern, indicative of minimal inter-symbol interference and robust timing synchronization, validating the system's capability to support 10 Gbps transmission over 20 km with high signal integrity.

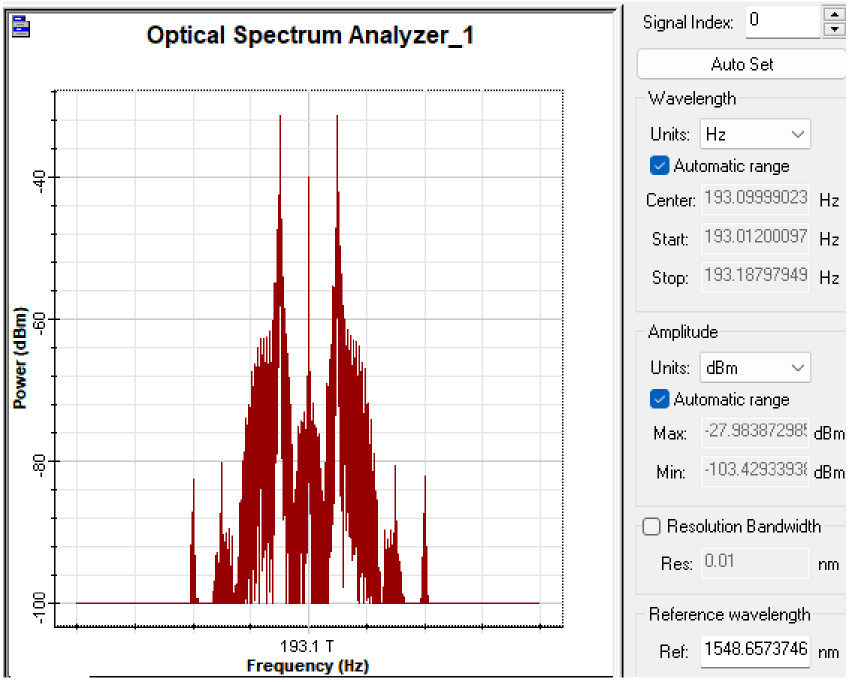

Figure 9: Spectrum of Output at Bessel Filter 1

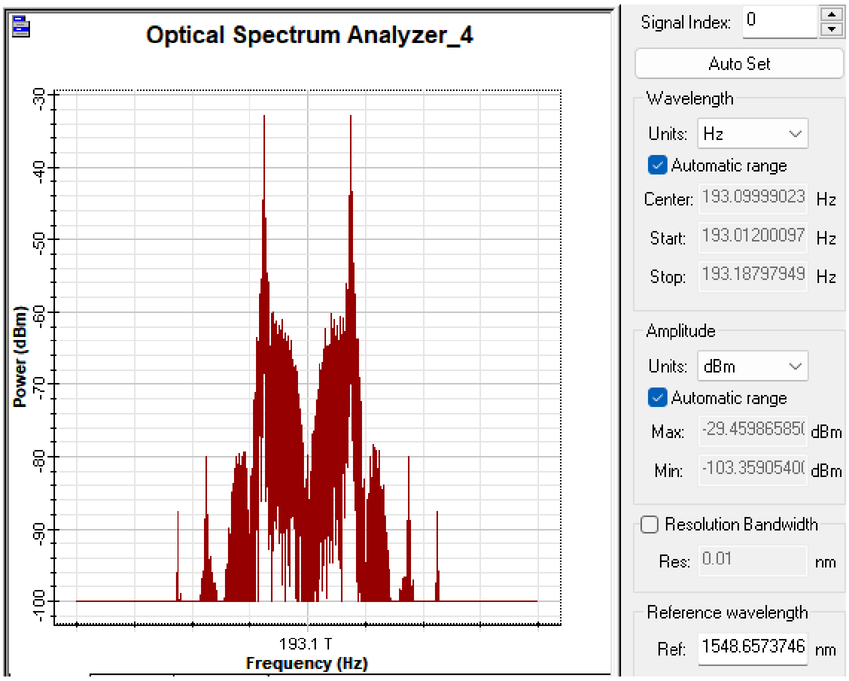

Figure 10: Spectrum of Output at Bessel Filter 2

Additional spectral observations from the Optical Spectrum Analyzer revealed multiple peaks in certain configurations, suggesting the presence of sidebands or potential wavelength-division multiplexing (WDM) components. The RF Spectrum Analyzer outputs confirmed the absence of significant spurious emissions, and the Optical Time Domain Visualizer displayed a stable power profile over time, indicating consistent transmission without temporal jitter. Overall, the simulation results demonstrate that the designed optical communication system achieves efficient modulation, low transmission loss, and reliable signal recovery, making it suitable for high-speed long-haul data transmission applications.

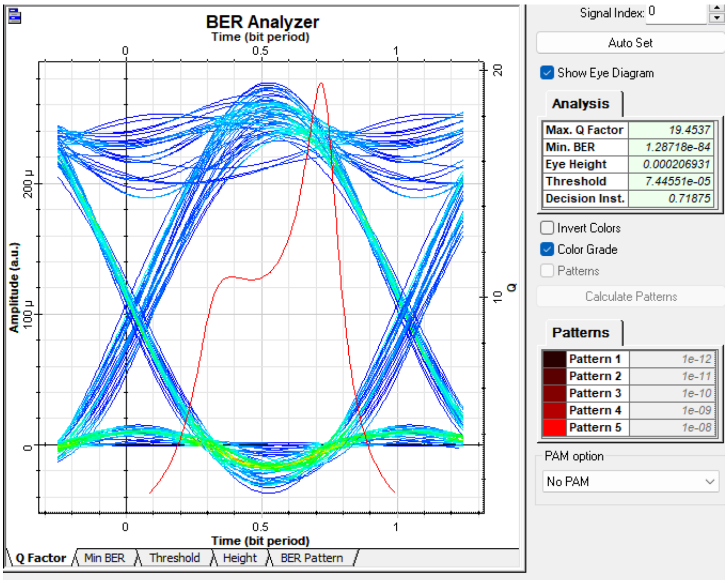

Figure 11: BER Output 1

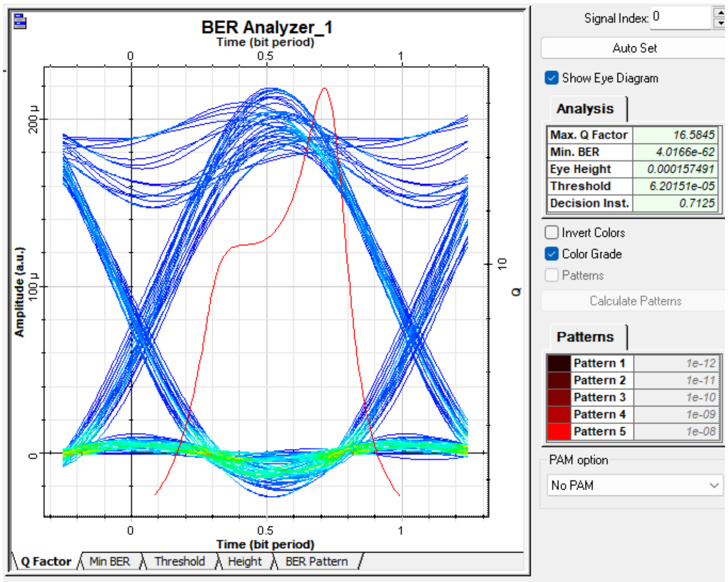

Figure 12: BER Output 2

Parameter	Value
Input Power	41.12 μW
Output Power at channel 1	292.47 μW
Output Power at channel 2	196.78 μW
Q-factor at channel 1	19.45
Q-factor at channel 2	16.58
BER at channel 1	1.28×10^{-84}
BER at channel 2	4.01×10^{-62}
Transmission Distance	20 km
System Frequency	28 GHz
Wavelength	1552.5 nm
Standard	ITU G-Sup39
Amplifier	SOA/EDFA
Gain of Amplifier	15 dB
Noise Figure of Amplifier	5 dB
Bandwidth	3 nm

Table 1: Results of the Proposed RoF System

The obtained results demonstrate the strong performance of the proposed Radio-over-Fibre (RoF) system operating at 28 GHz over a 20 km transmission link. The presence of the optical amplifier significantly enhances the received signal levels, improving the output power to 292.47 μW and 196.78 μW for channel 1 and channel 2 respectively, compared to the initial input power of just 41.12 μW. This improvement confirms that the amplifier not only compensates for fibre attenuation but also ensures efficient carrier transport over long distances. The high Q-factor values of 19.45 and 16.58 obtained for both channels indicate excellent signal quality with strong noise immunity.

Correspondingly, the BER values for both channels are extremely low on the order of 10^{-84} and 10^{-62} demonstrating error-free transmission performance and reliable data recovery at the receiver. Even with consideration of dispersion and amplifier noise, the system remains highly stable and efficient across the 3 nm bandwidth. Overall, these performance metrics validate that the designed RoF system meets the ITU G-Sup39 standard requirements and effectively supports 5G fronthaul transmission with minimal degradation, making it suitable for high-capacity and future-proof wireless network deployments.

CHAPTER 5: Conclusion and Future work

To conclude, Based on the simulation outputs and analyzer interfaces provided, the optical communication system demonstrates strong performance across both spectral and temporal domains. The Optical Spectrum Analyzer consistently reveals sharp peaks around 1.55 µm, confirming stable laser operation and effective modulation, while multiple peaks suggest potential for multi-wavelength transmission or sideband generation. RF Spectrum Analyzer results show dominant low-frequency signals with minimal spurious emissions, indicating clean modulation. The Optical Time Domain Visualizer displays a flat power profile, affirming temporal stability and jitter-free transmission. Collectively, these results validate the system's capability to support high-speed, long-distance communication with reliable signal integrity, making it well-suited for next-generation fiber-optic networks.

The future scope of Radio-over-Fiber (RoF) systems lies in their potential to support ultra-reliable, high-capacity, and energy-efficient communication infrastructures for beyond 5G and even 6G networks. With the growing demand for data-intensive applications such as augmented reality, autonomous vehicles, and massive IoT connectivity, RoF must evolve to deliver both scalability and robustness. One promising direction is the integration of RoF links with advanced photonic integrated circuits (PICs), which can significantly reduce the size, cost, and power consumption of optical front-haul networks.

Finally, as sustainability becomes a critical global objective, future RoF research will also need to prioritize energy efficiency. Innovations in low-power optical devices, eco-friendly materials, and green network architectures will help minimize the carbon footprint of next-generation communication systems.

References

1. M. H. C. Garcia et al., “A Tutorial on 5G NR V2X Communications,” IEEE Communications Surveys & Tutorials, vol. 23, no. 3, pp. 1972–2026, Third Quarter 2021, doi: 10.1109/COMST.2021.3057017.

2. R. Q. Shaddad et al., “Planning of 5G Millimeterwave Wireless Access Network for Dense Urban Area,” 2019 First International Conference of Intelligent Computing and Engineering (ICOICE), Hadhramout, Yemen, 2019, pp. 1–4, doi: 10.1109/ICOICE48418.2019.9035183.

3. C. Ranaweera, E. Wong, A. Nirmalathas, C. Jayasundara and C. Lim, “5G C-RAN With Optical Fronthaul: An Analysis From a Deployment Perspective,” Journal of Lightwave Technology, vol. 36, no. 11, pp. 2059–2068, Jun. 1, 2018, doi: 10.1109/JLT.2017.2782822.

4. S. S. P. Nugroho, Y. Natali and C. Apriono, “Design of Millimeter Wave based Radio over Fiber for 5G Applications,” 2022 1st International Conference on Information System & Information Technology (ICISIT), Yogyakarta, Indonesia, 2022, pp. 409–414, doi: 10.1109/ICISIT54091.2022.9872765.

5. A. P. Fatikah, Y. Natali and C. Apriono, “Bidirectional Radio Over Fiber with Millimeter Wave to Support 5G Fronthaul Network,” 2023 IEEE International Conference on Communication, Networks and Satellite (COMNETSAT), Malang, Indonesia, 2023, pp. 386–390, doi: 10.1109/COMNETSAT59769.2023.10420665.

6. A. Mumtaz, Y. Natali and C. Apriono, “Design of a WDM system with radio over free space optics for 5G fronthaul networks in an urban area,” International Conference on Green Energy, Computing and Intelligent Technology (GEn-CITy 2023), Iskandar Puteri, Malaysia, 2023, pp. 7–11, doi: 10.1049/icp.2023.1754.

7. A. Wahyudin, A. Hikmaturokhman and D. Ahmad Harish, “Spectrum Fee License Analysis on 3.5, 26, and 28 GHz Frequency For 5G Implementation in Indonesia,” 2021 IEEE International Conference on Communication, Networks and Satellite (COMNETSAT), Purwokerto, Indonesia, 2021, pp. 274–279, doi: 10.1109/COMNETSAT53002.2021.9530804.